HHS Public Access

Author manuscript

Oncogene. Author manuscript; available in PMC 2014 March 12.

Published in final edited form as:

Oncogene. 2013 September 12; 32(37): 4448–4456. doi:10.1038/onc.2012.443.

NBN Phosphorylation regulates the accumulation of MRN and ATM at sites of DNA Double-Strand Breaks

Jie Wen, Ph.D.[1], **Karen Cerosaletti, Ph.D.**[2], **Katherine J. Schultz**[3], **Jocyndra A. Wright**[1], and **Patrick Concannon, Ph.D.**[1,4]

[1]Department of Biochemistry and Molecular Genetics, University of Virginia, Charlottesville, VA, United States, 22908

[2]Translational Research Program, Benaroya Research Institute, 1201 Ninth Avenue, Seattle, WA, 98101

[3]School of Medicine, University of New Mexico, Albuquerque, NM, 87131

[4]Center for Public Health Genomics, University of Virginia, Charlottesville, VA, United States, 22908

Abstract

In response to ionizing radiation, the MRE11/RAD50/NBN (MRN) complex re-distributes to the sites of DNA double strand breaks (DSBs) where each of its individual components is phosphorylated by the serine-threonine kinase, ATM. ATM phosphorylation of NBN is required for activation of the S-phase checkpoint, but the mechanism whereby these phosphorylation events signal the checkpoint machinery remains unexplained. Here, we describe the use of direct protein transduction of the homing endonuclease, I-*Ppo*I, into human cells to generate site-specific DSBs. Direct transduction of I-*Ppo*I protein results in rapid accumulation and turnover of the endonuclease in live cells, facilitating comparisons across multiple cell lines. We demonstrate the utility of this system by introducing I-*Ppo*I into isogenic cell lines carrying mutations at the ATM phosphorylation sites in *NBN* and assaying the effects of these mutations on the spatial distribution and temporal accumulation of NBN and ATM at DSBs by chromatin immunoprecipitation, as well as timing and extent of DSB repair. Although the spatial distribution of NBN and ATM recruited to the sites of DSBs was comparable between control cells and those expressing phosphorylation mutants of NBN, the timing of accumulation of NBN and ATM was altered. Serine to alanine mutations that blocked phosphorylation resulted in delayed recruitment of both NBN and ATM to DSBs. Serine to glutamic acid substitutions that mimicked the phosphorylation event resulted in both increased and prolonged accumulation of both NBN and ATM at DSBs. The repair of DSBs in cells lacking full-length NBN was significantly delayed compared to control cells while blocking phosphorylation of NBN resulted in a more modest delay in repair. These data indicate

Corresponding Author: Patrick Concannon, Center for Public Health Genomics, University of Virginia, P.O. Box 800717, Charlottesville, VA 22908, pjc6n@virginia.edu, Tel: (434) 982-3288, Fax: (434) 924-1312.

Conflict of Interest: The authors declare no conflicts.

that following the induction of DSBs, phosphorylation of NBN regulates its accumulation, and that of ATM, at sites of DNA DSB as well as the timing of the repair of these sites.

Keywords

MRN; ATM; nibrin (NBN); I-*Ppo*I; DNA double-strand breaks

Introduction

Nijmegen Breakage Syndrome (NBS) is a rare autosomal recessive disorder characterized by growth retardation, microcephaly, immunodeficiency, and elevated cancer incidence (1–3). NBS results from biallelic hypomorphic mutations in the *NBN* gene, which encodes the 754 amino acid protein, Nibrin (3–5). The majority of NBS patients have truncating mutations in both alleles of the *NBN* gene. As a result, their cells fail to make detectable full-length NBN but can produce varying amounts of truncated fragments from the amino and carboxy terminal ends of the protein (6,7). *In vitro*, cells from NBS patients display impaired survival and an inability to activate the S-phase checkpoint after exposure to agents, such as ionizing radiation, that generate DNA DSBs (8,9). These phenotypes are also observed in cells from patients with Ataxia-Telangiectasia (A-T) which arises from deleterious mutations in the serine-threonine kinase ATM (10).

NBN associates constitutively with the MRE11 and RAD50 proteins to form the MRN complex (4,11). Knockouts of any of the components of the MRN complex in mice lead to early embryonic lethality (12–14), reflecting the essential role of this complex in DNA replication. While MRE11 and RAD50 play predominantly enzymatic roles in the complex, NBN plays a primarily regulatory role, directing the nuclear localization of the complex, re-distribution of the complex to DSBs upon exposure to DNA damaging agents, and stimulating the activities of the other components (15–19). The MRN complex associates with DNA DSBs within minutes following their formation (20,21), and contributes to recruitment of ATM to DNA DSBs through direct protein-protein interaction between ATM and the C-terminal end of NBN (22,23).

ATM becomes activated in the presence of DNA DSBs and phosphorylates a large number of substrates, some of which, like the components of the MRN complex, accumulate at the sites of DSBs (24–28). ATM phosphorylates NBN on as many as three serine residues (positions 278, 343, and 397) in response to DNA damage (29–32). Alanine substitutions at any one of these positions partially abrogate the S-phase cell cycle checkpoint, resulting in a phenotype of radio-resistant DNA synthesis (RDS) (33). However, the precise mechanism by which phosphorylation at these sites signals to the checkpoint machinery remains unknown.

In the current study, we utilize I-*Ppo*I, a eukaryotic homing endonuclease, to create DNA DSBs at defined endogenous sites in isogenic cell lines bearing different mutations at the phosphorylation sites in NBN, allowing us to track and compare protein recruitment and loss at or around these breaks by chromatin immunoprecipitation (ChIP) while also monitoring the repair of DSBs via quantitative PCR. Our data indicate that NBN phosphorylation

regulates the stabilization and/or accumulation of NBN or ATM at the sites of DSBs as well as the timing of repair at these sites.

Results

Purified I-*Ppo*I can be efficiently delivered to cells by protein transduction

Berkovich et al. previously described a human cell line engineered to express a tamoxifen-regulated version of I-*Ppo*I allowing the induction of DNA DSBs at I-*Ppo*I sites on chromosomes 1 and 8 and characterization of the DNA damage response at these sites by ChIP (34). In order to facilitate the comparison of the I-*Ppo*I response across multiple cell lines, and limit the length of exposure of cells to the nuclease, we developed a protein transduction approach for the expression of I-*Ppo*I in human cells using cell penetrating peptides (CPP) (35,36). CPP have been shown to deliver a range of different cargoes, including proteins, drugs, nucleic acids and imaging reagents to a wide array of cell types with generally high efficiency, potentially allowing the application of I-*Ppo*I to a variety of different cell lines. A gene encoding I-*Ppo*I was chemically synthesized, cloned, and its protein product was affinity purified from *E. coli* (Fig. 1A). Overnight incubation of purified I-*Ppo*I with a linearized plasmid containing the 15 base pair I-*Ppo*I recognition sequence confirmed the activity and specificity of the enzyme and the absence of other significant endonuclease activities (Fig. 1B). CPP incorporating a nuclear localization signal were then used to introduce the purified I-*Ppo*I into an SV40 transformed fibroblast cell line from an NBS patient (NBS-ILB1 cells) (37) stably transfected with either the wild-type *NBN* gene (ILB1-[NBN] cells), NBN with alanine substitutions at S278 and S343 (ILB1-[NBN-S>A] cells) or the empty retroviral vector (ILB1 cells). I-*Ppo*I protein of the expected molecular weight was detected in each of these cell lines as early as 1 hour post transduction (Fig. 1C) and localized predominantly to the nucleus at all time points tested (Fig. 1D). No significant differences between cell lines were observed in the uptake or subsequent loss of I-*Ppo*I by Western blot.

Transduced I-*Ppo*I induces site-specific DNA cleavage in vivo

A BLAST search of the human genome reference sequence (hg19) identified 10 sites of sequence identity to the I-*Ppo*I restriction site. In addition to the previously reported sites on chromosome 1 within the *DAB1* gene and chromosome 8 within the ribosomal DNA cluster (34), sites were identified on chromosome 1, 2, 3, 7, 11, X, Y and in an unaligned segment. In order to assess the activity of transduced I-*Ppo*I, ILB1-[NBN] cells were transduced with I-*Ppo*I and quantitative PCR was performed with primers spanning each of these putative cleavage sites. The yield of PCR product from each of these sites at different time points post-transduction was compared with that from a reference sequence that did not contain an I-*Ppo*I site (Fig. 2A). In three independent experiments, eight of the 10 sites displayed cutting upon transduction with I-*Ppo*I, as evidenced by yields less than 100%, but the maximum cutting never exceeded 30% for any site.

A more extensive time course experiment was performed at a single site utilizing ILB1, ILB1-[NBN], ILB1-[NBN-S>A], ILB1-[NBN-S>E] and 411BRneo cells. ILB1-[NBN-S>A], which has been previously described (38), expressed NBN with S>A mutations at

positions 278 and 343. ILB1-[NBN-S>E], newly generated for the current study, expressed NBN with S>E mutations at positions 278, 343, and 397. The 411BRneo cell line lacks detectable ligase IV activity due to a homozygous missense mutation at a highly conserved residue (R278H) (39). If the limited cleavage by I-*Ppo*I observed is the result of repair of these sites by non-homologous end-joining, then the 411BRneo cells might be expected to display enhanced cutting in this assay. However, the cutting by I-*Ppo*I in 411BRneo cells was not significantly greater than what was observed in any of the ILB1 derived cell lines, although repair was not complete even 24 hours after transduction with I-*Ppo*I. I-*Ppo*I sites in ILB1-[NBN] and ILB1-[NBN-S>A] cells were fully repaired by 8 hours although the ILB1-[NBN-S>A] cells lagged behind the ILB1-[NBN] cells at the 5 hour time point. ILB1 cells, which lack full-length NBN, and ILB1-[NBN-S>E] cells required a more prolonged time period to complete repair (Fig. 2B). The maximal cutting did not exceed 30% in any of these fibroblast cell lines. Similar limitations on the maximum extent of cutting were observed in cell lines of other origins such as HEK293T and a B-lymphoblastoid cell line, 309, despite successful transduction of I-*Ppo*I into these cell lines using CPP (Fig. 2C).

I-*Ppo*I protein transduction activates ATM-dependent DNA damage responses

Figure 3A shows the activation of ATM, as assayed by phosphorylation on serine 1981 after treatment of ILB1 and ILB1-[NBN] cells with I-*Ppo*I. As expected, phosphorylation of ATM is attenuated at early time points in ILB1 cells where full length NBN is absent, whereas S1981 phosphorylation was detected at 1 hour and was still present at 3 hours in complemented ILB1-[NBN] cells (Fig. 3A, upper panel). Phosphorylation of NBN on serine 343 by activated ATM is similarly observed in ILB1-[NBN] cells (Fig. 3A, lower panel).

Activated ATM phosphorylates histone H2AX at the sites of DNA damage forming γH2AX (40). A ChIP assay using antibodies directed against γH2AX and amplification primers adjacent to the I-*Ppo*I site on chromosome 1 in the *DAB1* gene revealed that γH2AX could be detected at this site by 1 hour after I-*Ppo*I protein transduction (Fig. 3B). Immunofluorescent microscopy revealed γH2AX staining in a majority (>90%) of the cells treated with I-*Ppo*I (Fig. 3C, low resolution panel) and damage foci in individual cells consistent with the number of known I-*Ppo*I sites in the human genome (Fig. 3C, high resolution panel).

ATM phosphorylation of NBN facilitates its accumulation at sites of DNA damage

To assess the role of ATM phosphorylation of NBN on the timing and spatial distribution of its accumulation at DNA DSBs, two different transfected versions of ILB1 cells were utilized, ILB1-[NBN-S>A] and ILB1-[NBN-S>E] cells. In comparison to ILB1 cells transfected with a wild type NBN construct, both cell lines expressed comparable levels of NBN and neither was significantly impaired in survival following exposure to ionizing radiation (Supplementary Figures 1 and 2). To assay the recruitment and distribution of proteins at and around a site-specific DSB in these cell lines, we utilized pairs of primers for ChIP analysis spaced up to 20kb on either side of the I-*Ppo*I site located within the *DAB1* gene on chromosome 1 and assayed for protein accumulation from 1 to 8 hours after treatment of cells with I-*Ppo*I. In ILB1 cells, NBN could not be detected by ChIP at any time point (Fig. 4A, first panel). In ILB1-[NBN] cells, NBN was detected at the cleavage

site within 1 hour after transduction, peaking at 3 hours and then decreasing by 5 hours. At later time points, the accumulation of NBN shifted to sites from 3–10kb flanking the DSB (Fig. 4A, second panel). In ILB1-[NBN-S>A] cells, the accumulation of NBN at the cleavage site was delayed relative to wild type, peaking at 5 hours followed by the normal decline and shift to distal sites by 8 hours (Fig. 4A, third panel). In ILB1-[NBN-S>E] cells, the accumulation of NBN at the cleavage site was comparable to wild type at the 3 hours time point but then failed to resolve, continuing to increase until a broad accumulation of NBN at, and around the cleavage site was apparent at the latest time point, 8 hours (Fig. 4A, fourth panel).

Since ATM recruitment to the sites of DNA damage is stimulated at early times after DNA damage induction by its interaction with the carboxy terminal end of NBN (23), the ChIP assay was also used to examine ATM protein recruitment to the I-*Ppo*I cut site. Whereas NBN accumulated directly at the DNA DSB site, ATM was detected in regions of 3–10kb flanking the site, similar to the accumulation of NBN after 5h (Fig. 4B). In ILB1 cells there was a very modest increase in the amount of ATM present at these sites over time, consistent with the evidence that NBN stimulates the activation of ATM but is not obligatory for its activation (Fig. 4B, first panel) (38,41–45). In ILB1-[NBN] cells, robust ATM accumulation on both sides of the DSB was observed by 1 hour after I-*Ppo*I transfection decreasing thereafter (Fig. 4B, second panel). As was observed for NBN, in ILB1-[NBN-S>A] cells, ATM accumulation at the I-*Ppo*I cut site was delayed relative to ILB1-[NBN] cells. ATM was undetectable at 1 hour and did not peak until around 5 hours after I-*Ppo*I transfection before declining (Fig. 4B, third panel). ATM accumulation in ILB1-[NBN-S>E] cells similarly mirrored the results for NBN accumulation with this mutant, reaching wild type levels at 3 hours but then continuing to accumulate out to 8 hours instead of declining as was observed for wild type NBN (Fig. 4B, fourth panel).

While ATM accumulation at the site of the induced DNA DSB was altered in ILB1-[NBN-S>A] and ILB1-[NBN-S>E] cells, the amount of activated ATM in the cells, assayed by phosphorylation on S1981, was generally indistinguishable from that in ILB1-[NBN] cells at 1, 3 and 8 hours (Fig. 5A), with the possible exception of a slightly elevated basal level of S1981 phosphorylation in the ILB1-[NBN-S>E] cells. Phosphorylation of CHEK2 on T68 (46) at the same time points was indistinguishable from wild type (Fig. 5B). An additional substrate, SMC1, which is phosphorylated by ATM on S957 (44), phosphorylation in the ILB1-[NBN-S>E] cells was increased at the 1 hour time point relative to the other cell lines (Fig. 5C).

Discussion

The exact role of ATM phosphorylation of NBN in the DNA damage response remains unresolved. Serine to alanine substitutions at the known ATM phosphorylation sites on NBN have, at best, only modest effects on cell survival after irradiation (47–50). These mutations do confer a phenotype of radio-resistant DNA synthesis but the mechanism whereby phosphorylation on these residues signals to the S-phase checkpoint machinery has not been elucidated. There is no evidence for modification-dependent protein interactions at the residues on NBN that are phosphorylated by ATM.

In the current study we examined the spatial orientation and timing of recruitment of NBN and ATM to the sites of DNA breaks induced in isogenic cell lines expressing no full length NBN, wild type NBN or NBN in which the ATM phosphorylation sites had been mutated to alanine or glutamic acid in order to determine if there were features of the spatio-temporal response to DNA damage that were dependent upon ATM mediated phosphorylation of NBN. Prior studies have explored this issue using laser micro-irradiation in live cells followed by confocal microscopy (20,51,52). To obtain a higher level of resolution than available via microscopy we adopted a restriction enzyme-driven ChIP-based approach. The approach of using restriction endonucleases, such as I-*Ppo*I used here, to induce DNA DSBs in mammalian cells and the subsequent application of ChIP to these sites is not novel (34,53,54), but in previous implementations these approaches have relied upon transfection of the gene encoding the restriction enzyme or the creation of cell lines in which the restriction enzyme was under the control of an inducible promoter. Such implementations carry with them particular challenges including over-expression or prolonged exposure to the restriction enzyme in the case of transient transfection and the need to individually engineer cell lines carrying different mutations in the case of inducible promoters. Nevertheless, Berkovich et al. were able to use a modified I-*Ppo*I construct whose nuclear localization could be induced in transfected cells with tamoxifen, to demonstrate the recruitment of ATM and NBN to the I-*Ppo*I site on chromosome 1 and the concomitant loss of histone H2B at this site.

In the approach described here, we employ cell penetrating peptides to introduce bacterially-produced and epitope-tagged I-*Ppo*I protein into human cells bearing different site specific mutations in DNA damage response genes. We demonstrate that under the conditions utilized, the majority of cells (>90%) are transduced with the protein, incur site specific DNA DSBs and initiate a normal DNA damage response to the presence of these DSBs. Eight of 10 putative I-*Ppo*I restriction sites identified in the human genome by sequence analysis displayed evidence of cutting by the exogenously introduced endonuclease. Upon transduction of cells with I-*Ppo*I complexed with cell penetrating peptides, site-specific cleavage of DNA was detected 1 hour after transduction (the earliest time point assayed) and was fully repaired within 8 hours. While the majority of cells treated with I-*Ppo*I incur some DNA DSBs, as evidenced by positive staining for γH2AX, the maximum cutting, per individual site, did not exceed 30%. Mutations in proteins involved in DNA damage sensing or repair affected the time to complete repair but not the maximum cutting, suggesting that repeated cycles of cutting and repair were probably not a major factor in determining maximum cutting level. In I-*Ppo*I transduced ILB1-[NBN] cells the profile of endonucleolytic cutting and repair tracked slightly behind the measures of I-*Ppo*I levels, which peaked at one hour and declined thereafter. Only limited amounts of I-*Ppo*I were detected after 5 hours by immunoblot or immunofluorescence. In ILB1 cells which lack full-length NBN, and in 411BRneo cells that lack ligase IV, repair was significantly delayed. ILB1 cells ultimately rejoined the induced DSBs while in 411BRneo cells more than half of the cut sites remained unrepaired after 24 hours.

The different genomic sites tested in the cutting assay include sites within genes and in intergenic and even highly repetitive regions which are likely to differ in chromatin

configuration. We observed no consistent differences between, for example, genic and intergenic sites, in the maximum levels of cutting attained, but the variability between different cut sites suggests that the role of chromatin in this process bears further investigating. We also observed similar results in cell lines of different origins, such as HEK293 cells or B lymphoblastoid cells. It is possible that preparations of the I-*Ppo*I enzyme with varying specific activities may differ in the maximum extent of cutting, but, to date, we have observed no significant differences among the preparations we have made (data not shown).

To explore the effects of ATM phosphorylation of NBN on the accumulation of these proteins at the sites of DNA DSBs, we applied the I-*Ppo*I transduction system to two mutant cell lines, ILB1-[NBN-S>A] cells, a previously described line with serine to alanine substitutions at ATM phosphorylation sites in NBN, and ILB1-[NBN-S>E] cells, a new line in which these residues were changed to glutamic acid to mimic constitutive phosphorylation. We observed significant effects on both the timing of repair and the accumulation of ATM and NBN at I-*Ppo*I sites in these mutants, but these effects did not result in impaired survival in clonogenic assays. In ILB1-[NBN-S>A] cells the time course of repair of I-*Ppo*I-induced DNA DSBs was delayed at 5 hours relative to that observed in ILB1 cells complemented with wild type NBN, but was still complete by 8 hours. Blocking the phosphorylation of NBN on these sites also had a substantial effect on the accumulation of NBN in the vicinity of the I-*Ppo*I-induced DSB in the *DAB1* gene on chromosome 1 as well as the accumulation of ATM at the same site. Interestingly, in ILB1-[NBN-S>E] cells the time course of repair of I-*Ppo*I-induced DNA DSBs was more severely delayed relative to that in ILB1-[NBN] cells, although still complete by approximately 18 hours. ILB1-[NBN-S>E] cells displayed normal accumulation of NBN and ATM at the I-*Ppo*I site, but the proteins failed to dissociate from the site, as observed for ILB1-[NBN] cells, and displayed continued accumulation.

In general, the spatial distribution of NBN and ATM at the DSB site in our ChIP assays was indistinguishable in ILB1 cells complemented with wild type NBN and the S>A or S>E mutant, as was the extent of ATM activation; it was only the timing of accumulation that was affected. This spatial pattern of NBN and ATM accumulation was also consistent with that observed by Berkovitch et al. (34) although it is unclear how well the time points at which observations were made in the two different systems correspond. Our results suggest that the main effect of ATM phosphorylation of NBN is to stabilize the protein at the site of the DSB leading to its accumulation and that of ATM. In the absence of phosphorylation, both NBN and ATM still accumulate but with slower kinetics. When phosphorylation of NBN is enhanced via phospho-mimic amino acid substitutions, accumulation of both NBN and ATM at the DSB site is similarly enhanced, in particular by the failure of these proteins to dissociate from the site in a timely fashion, as observed in cells expressing wild-type NBN. Paradoxically, this enhanced accumulation is associated with delayed repair of the site. However, based upon observations of the timing of accumulation of XRCC4 at the sites of DSBs, Berkovich et al. (34) speculated that it was necessary for repair proteins to displace signaling proteins, such as ATM, from the cut site at late time points in order to carry out repair. It is tempting to speculate that the mutant form of NBN in ILB1-[NBN-S>E] cells,

whose dissociation from the site is impaired, may hinder access of repair proteins to the DSB and thus, delay repair. A major benefit of the ChIP system described here is that the effects of mutations such as this on the spatio-temporal features of the cellular response to DNA DSBs are both readily observable and comparable between cell lines even in cases where classical assays, such as clonogenic survival, cannot discriminate between the different mutant cell lines.

Materials and methods

Protein purification

I-*Ppo*I open reading frame was chemically synthesized (GenScript USA Inc. Piscataway, NJ) and cloned into the pUC57 vector. The insert was excised with *Not*I and *Xho*I and ligated into a compatible vector, pET45b (+) (Novagen, EMD Chemicals, Inc. Gibbstown, NJ). This resulted in the addition of a 6-histidine epitope tag to the N-terminus of the I-*Ppo*I open reading frame, and brought its expression under the control of a T7 RNA polymerase. I-*Ppo*I protein expression was induced by IPTG (Fisher Scientific, Pittsburgh, PA) in *E. coli* strain BL21-DE3 (Novagen). Cultures were allowed to grow 6–8 hours at 37°C, and then lysed in lysis buffer. The cell lysate was stored in −80°C overnight and thawed on ice before protein purification. The lysate was then passed through French Press Cell Disruptor twice and cell debris was removed by centrifugation. The resulting supernatant was incubated with Ni-NTA beads (Qiagen Inc., Valencia, CA) for 30min with agitation at 4°C, then loaded onto a poly-prep chromatography column (Bio-Rad, Hercules, CA). The protein was eluted by an increasing gradient of imidazole (Fisher). The fractions containing I-*Ppo*I were pooled together and dialyzed overnight at 4°C. Protein concentration was determined using Bio-Rad protein assay (Bio-Rad). Purified protein was resolved on a NuPAGE gradient 4–12% Bis-Tris Gel (Invitrogen, Grand Island, NY) and stained using EZBlue Gel Staining Reagent (Sigma-Aldrich Product, St. Louis, MO).

Cell culture and protein transduction

All ILB1 derived cells were grown in Dulbecco's Modified Eagle's Medium (DMEM) supplemented with 10% fetal bovine serum (FBS), 1% pen/strep, 1% nonessential amino acid (NEAA), 1% sodium pyruvate, and 0.5mg/ml geneticin. 411BRneo cells were cultured in Minimum Essential Medium (MEM) supplemented with 15% FBS, 1% pen/strep, 1% NEAA, and 1% sodium pyruvate. HEK293T cells were cultured in DMEM supplemented with 10% FBS, 1% pen/strep, 1% NEAA and 1% sodium pyruvate. BLCL-309 cells were cultured in MEM with 10% FBS, 1% pen/strep, 1% NEAA and 1% sodium pyruvate. For all experiments, cells were maintained at 37°C in 5% CO_2/95% air. I-*Ppo*I protein was introduced into target cell lines using either cell penetrating peptide (CPP), Pep-1, (AnaSpec, Fremont, CA) or protein delivery reagent, Chariot (Active Motif, Carlsbad, CA). No significant differences were observed between the transfection efficiency of Pep-1 and Chariot. I-*Ppo*I protein transfection was performed according to the manufacturer's instructions. First, I-*Ppo*I protein was diluted in PBS and Pep-1/chariot was diluted in sterile water. Then the diluted I-*Ppo*I was added to the diluted Pep-1/chariot and incubated at room temperature for 30min to allow the protein/CPP complex to form. Before transfection, cells

were washed once with PBS and overlaid with I-*Ppo*I/CPP complex. Serum-free medium was added to the cell culture, which was then incubated at 37°C for at least 1 hour.

DNA cleavage assay

Cells were grown in 10cm dishes to approximately 95% confluence. After I-*Ppo*I protein transduction, cells were washed twice with ice-cold PBS and harvested in ice-cold PBS containing protease inhibitors (Roche Diagnostics, Indianapolis IN). After centrifugation at 3000rpm for 5min, the supernatant was removed and cells were resuspended in ChIP sonication buffer containing protease inhibitors, incubated on ice for 10min, and subjected to sonication using a Branson Sonifier 250 at output 8.0 and 80% cycle duty for 90s. After sonication, cell suspensions were centrifuged at 13,000rpm for 15min, and supernatant was collected as whole cell extracts (WCE). DNA was extracted from equal amount of WCE using PCR purification kit (Qiagen). Aliquots (5μl) were used for each real-time PCR reaction with primers spanning each of the putative I-*Ppo*I cleavage sites and a reference sequence that did not contain an I-*Ppo*I site. Primer sequences are provided in Supplementary Table 1. PCR results were analyzed by comparing the yield of PCR product from each of these sites at different time points post-transduction with that from the reference sequence. Ct values were calculated and represented as a percentage of uncut I-*Ppo*I sites. Experiments were repeated three times, and the error bars represent mean ± SD.

Immunoblotting and immunoprecipitation

For immunoblotting, cells were lysed in SDS lysis buffer with protease and phosphatase inhibitors (Roche). Nuclear and cytoplasmic extracts were prepared using NE-PER Nuclear and Cytoplasmic Extraction Reagents (Thermo Scientific, Rockford, IL). Protein concentration was determined using Bio-Rad protein assay (Bio-Rad). Whole cell lysates or nuclear extracts containing 50μg of protein were separated on gradient NuPAGE (3–8% Tris-Acetate or 4–12% Bis-Tris) Gels (Invitrogen) and transferred to Immobilon-P transfer membranes (Millipore Corporation, Billerica, MA) for antibody probing. For immunoprecipitation, cells were lysed in EBC buffer with protease and phosphatase inhibitors. Lysates containing 500μg of protein were incubated with indicated antibody overnight at 4°C, and protein G agarose (Santa Cruz) was added for an additional 1 hour at 4°C. Agarose pellets were washed three times in EBC buffer, and the bound proteins were removed by boiling in LDS buffer (Invitrogen). Eluted proteins were then separated on a 3–8% Tris-Acetate gel and transferred to Immobilon-P transfer membrane for antibody probing. Antibodies used were: anti-ATM (Genetex Inc. Irvine, CA), anti-ATMSer1981p (Rockland Immunochemicals, Inc. Gilbertsville, PA), anti-NBN (Novus Biologicals, Inc., Littleton, CO), anti-NBNSer343p (Upstate Cell Signaling Solutions, Lake Placid, NY), anti-γH2AX (Millipore), anti-His (GE Healthcare, Piscataway, NJ), anti-tubulin (Sigma-Aldrich Product), anti-CHK2Thr68p (Cell Signaling Technology), anti-CHK2 (Novus Biolgocals, Inc.), anti-SMC1Ser957p (Cell Signaling Technology), anti-SMC1 (Bethyl Laboratories, Inc. Montgomery, TX), anti-Hsp90 (Cell Signaling Technology) and anti-p84 (Genetex).

Immunofluorescence microscopy

Cells were grown in a 4-well chamber slide system (Nalge Nunc International, Naperville, IL) to 50% confluence. After transfection, cells were fixed in 4% paraformaldehyde solution (Electron Microscopy Sciences, Hatfield, PA) for 20min at room temperature, followed by 5min permeabilization in 0.4% Triton X-100 solution (Sigma-Aldrich Product). After blocking in 10% BSA/PBS at 37°C for 30min, cells were incubated with anti-γH2AX antibody (Millipore) at 4°C overnight followed by incubation with Alexa Fluor 488-labeled anti-mouse antibody (Invitrogen) at room temperature for 1 hour. Slides were removed from chamber and air dried in dark for 5min before mounting with Vectashield Mounting Medium (with DAPI) (Vector Laboratories, Inc., Burlingame, CA).

Chromatin immunoprecipitation assay

Cells were grown in 15cm dishes to approximately 95% confluence. After protein transduction, cells were cross-linked with 1% formaldehyde for 10min at 37°C. Cross-linking was quenched by adding glycine to a final concentration of 0.125M. Cells were washed twice with ice-cold PBS and harvested in ice-cold PBS containing protease inhibitors. After centrifugation at 3000rpm for 5min, the supernatant was removed and cells were resuspended in ChIP sonication buffer containing protease inhibitors, incubated on ice for 10min, and then subjected to sonication using a Branson Sonifier 250 at an output of 3.0. Twenty-five cycles of 5s pulses were administered to shear chromatin to 700–1000bp fragments. The effectiveness of shearing was confirmed by testing DNA aliquot on agarose gel. After sonication, cell suspensions were centrifuged at 13,000rpm for 15min, and supernatant was collected as whole cell extracts (WCE). WCEs (0.2ml, corresponding to approximately 3×10^6 cells) were diluted to 1ml in ChIP sonication buffer and then incubated with either no antibody or antibodies targeting ATM or NBN. Another 0.2ml of the WCE was saved for later standard curve analysis. Incubations occurred overnight at 4°C with agitation. The next morning 45μl of protein G-agarose slurry (Santa Cruz Biotechnology) was added and incubated for another 2 hours at 4°C with agitation. The agarose beads were washed three times with ChIP sonication buffer and twice with TE buffer. DNA and protein were eluted from the pellets by incubating the pellets with 100μl of elution buffer. Cross-linking was reversed by incubating at 65°C for overnight. DNA fragments were extracted using PCR purification kit (Qiagen). Aliquots (5μl) were used for each real time PCR reaction to quantitate immunoprecipitated fragments. PCR results were analyzed from standard curve generated by input dilutions: from 100% to 0.0064%. Results represent the average from three individual experiments. Primer sequences are provided in Supplementary Table 1.

Supplementary Material

Refer to Web version on PubMed Central for supplementary material.

Acknowledgments

Supported by a grant from the NCI (CA57569) to P.C.

Reference List

1. Weemaes CMR, Hustinx TWJ, Scheres JMJC, van Munster PJJ, Bakkeren JAJM, Taalman RDFM. A new chromosomal instability disorder: the Nijmegen breakage syndrome. Acta Paediatr. 1981; 70:557–64.
2. Taalman RDFM, Hustinx TWJ, Weemaes CMR, Seemanova E, Schmidt A, Passarge E, et al. Further delineation of the Nijmegen breakage syndrome. Am J Med Genet. 1989; 32:425–31. [PubMed: 2786340]
3. Varon R, Vissinga C, Platzer M, Cerosaletti KM, Chrzanowska KH, Saar K, et al. Nibrin, a novel DNA double-strand break repair protein, is mutated in Nijmegen Breakage Syndrome. Cell. 1998; 93:467–76. [PubMed: 9590180]
4. Carney JP, Maser RS, Olivares H, Davis EM, Le Beau M, Yates JR III, et al. The hMre11/hRad50 protein complex and Nijmegen breakage syndrome: linkage of double-strand break repair to the cellular DNA damage response. Cell. 1998 May 1; 93(3):477–86. [PubMed: 9590181]
5. Matsuura S, Tauchi H, Nakamura A, Kondo N, Sakamoto S, Endo S, et al. Positional cloning of the gene for Nijmegen breakage syndrome. Nat Genet. 1998 Jun; 19(2):179–81. [PubMed: 9620777]
6. Maser RS, Zinkel R, Petrini JH. An alternative mode of translation permits production of a variant NBS1 protein from the common Nijmegen breakage syndrome allele. Nat Genet. 2001 Apr; 27(4): 417–21. [PubMed: 11279524]
7. Lins S, Kim R, Kruger L, Chrzanowska KH, Seemanova E, Digweed M. Clinical variability and expression of the NBN c.657del5 allele in Nijmegen Breakage Syndrome. Gene. 2009 Nov 1; 447(1):12–7. [PubMed: 19635536]
8. Taalman RDFM, Jaspers NGJ, Scheres JMJC, de Wit J, Hustinx TWJ. Hypersensitivity to inonizing radiation in vitro, a new chromosomal breakage disorder, the Nijmegen breakage syndrome. Mutat Res. 1983; 112:23–32. [PubMed: 6828038]
9. Jaspers NGJ, Taalman RDFM, Baan C. Patients with an inherited syndrome characterized by immunodeficiency, microcephaly, and chromosomal instability: genetic relationship to ataxia telangiectasia. Am J Hum Genet. 1988; 42:66–73. [PubMed: 3337113]
10. Savitsky K, Bar-Shira A, Gilad S, Rotman G, Ziv Y, Vanagaite L, et al. A single ataxia telangiectasia gene with a product similar to PI-3 kinase. Science. 1995 Jun 23; 268(5218):1749–53. [PubMed: 7792600]
11. Desai-Mehta A, Cerosaletti KM, Concannon P. Distinct functional domains of nibrin mediate Mre11 binding, focus formation, and nuclear localization. Mol Cell Biol. 2001 Mar; 21(6):2184–91. [PubMed: 11238951]
12. Luo G, Yao MS, Bender CF, Mills M, Bladl AR, Bradley A, et al. Disruption of mRad50 causes embryonic stem cell lethality, abnormal embryonic development, and sensitivity to ionizing radiation. Proc Natl Acad Sci U S A. 1999 Jun 22; 96(13):7376–81. [PubMed: 10377422]
13. Xiao Y, Weaver DT. Conditional gene targeted deletion by Cre recombinase demonstrates the requirement for the double-strand break repair Mre11 protein in murine embryonic stem cells. Nucleic Acids Res. 1997; 25:2985–91. [PubMed: 9224597]
14. Zhu J, Petersen S, Tessarollo L, Nussenzweig A. Targeted disruption of the Nijmegen breakage syndrome gene NBS1 leads to early embryonic lethality in mice. Curr Biol. 2001 Jan 23; 11(2): 105–9. [PubMed: 11231126]
15. Paull TT, Gellert M. Nbs1 potentiates ATP-driven DNA unwinding and endonuclease cleavage by the Mre11/Rad50 complex. Genes Dev. 1999 May 15; 13(10):1276–88. [PubMed: 10346816]
16. Paull TT, Gellert M. The 3′ to 5′ exonuclease activity of Mre 11 facilitates repair of DNA double-strand breaks. Mol Cell. 1998 Jun; 1(7):969–79. [PubMed: 9651580]
17. Lee JH, Ghirlando R, Bhaskara V, Hoffmeyer MR, Gu J, Paull TT. Regulation of Mre11/Rad50 by Nbs1: effects on nucleotide-dependent DNA binding and association with ataxia-telangiectasia-like disorder mutant complexes. J Biol Chem. 2003 Nov 14; 278(46):45171–81. [PubMed: 12966088]
18. de Jager M, van Noort J, van Gent DC, Dekker C, Kanaar R, Wyman C. Human Rad50/Mre11 is a flexible complex that can tether DNA ends. Mol Cell. 2001 Nov; 8(5):1129–35. [PubMed: 11741547]

19. Vissinga CS, Yeo TC, Warren S, Brawley JV, Phillips J, Cerosaletti K, et al. Nuclear export of NBN is required for normal cellular responses to radiation. Mol Cell Biol. 2009 Feb; 29(4):1000–6. [PubMed: 19075003]
20. Lukas C, Falck J, Bartkova J, Bartek J, Lukas J. Distinct spatiotemporal dynamics of mammalian checkpoint regulators induced by DNA damage. Nat Cell Biol. 2003 Mar; 5(3):255–60. [PubMed: 12598907]
21. Nelms BE, Maser RS, MacKay JF, Lagally MG, Petrini JH. In situ visualization of DNA double-strand break repair in human fibroblasts. Science. 1998 Apr 24; 280(5363):590–2. [PubMed: 9554850]
22. Falck J, Coates J, Jackson SP. Conserved modes of recruitment of ATM, ATR and DNA-PKcs to sites of DNA damage. Nature. 2005 Mar 31; 434(7033):605–11. [PubMed: 15758953]
23. Cerosaletti K, Wright J, Concannon P. Active role for nibrin in the kinetics of atm activation. Mol Cell Biol. 2006 Mar; 26(5):1691–9. [PubMed: 16478990]
24. Bakkenist CJ, Kastan MB. DNA damage activates ATM through intermolecular autophosphorylation and dimer dissociation. Nature. 2003 Jan 30; 421(6922):499–506. [PubMed: 12556884]
25. Matsuoka S, Ballif BA, Smogorzewska A, McDonald ER III, Hurov KE, Luo J, et al. ATM and ATR substrate analysis reveals extensive protein networks responsive to DNA damage. Science. 2007 May 25; 316(5828):1160–6. [PubMed: 17525332]
26. Di VM, Ying CY, Gautier J. PIKK-dependent phosphorylation of Mre11 induces MRN complex inactivation by disassembly from chromatin. DNA Repair (Amst). 2009 Nov 2; 8(11):1311–20. [PubMed: 19709933]
27. Dong Z, Zhong Q, Chen PL. The Nijmegen breakage syndrome protein is essential for Mre11 phosphorylation upon DNA damage. J Biol Chem. 1999 Jul 9; 274(28):19513–6. [PubMed: 10391882]
28. Gatei M, Jakob B, Chen P, Kijas AW, Becherel OJ, Gueven N, et al. ATM protein-dependent phosphorylation of Rad50 protein regulates DNA repair and cell cycle control. J Biol Chem. 2011 Sep 9; 286(36):31542–56. [PubMed: 21757780]
29. Lim DS, Kim ST, Xu B, Maser RS, Lin J, Petrini JH, et al. ATM phosphorylates p95/nbs1 in an S-phase checkpoint pathway. Nature. 2000 Apr 6; 404(6778):613–7. [PubMed: 10766245]
30. Wu X, Ranganathan V, Weisman DS, Heine WF, Ciccone DN, O'Neill TB, et al. ATM phosphorylation of Nijmegen breakage syndrome protein is required in a DNA damage response. Nature. 2000 May 25; 405(6785):477–82. [PubMed: 10839545]
31. Gatei M, Young D, Cerosaletti KM, Desai-Mehta A, Spring K, Kozlov S, et al. ATM-dependent phosphorylation of nibrin in response to radiation exposure. Nat Genet. 2000 May; 25(1):115–9. [PubMed: 10802669]
32. Zhao S, Weng YC, Yuan SS, Lin YT, Hsu HC, Lin SC, et al. Functional link between ataxia-telangiectasia and Nijmegen breakage syndrome gene products. Nature. 2000 May 25; 405(6785): 473–7. [PubMed: 10839544]
33. Falck J, Petrini JH, Williams BR, Lukas J, Bartek J. The DNA damage-dependent intra-S phase checkpoint is regulated by parallel pathways. Nat Genet. 2002 Mar; 30(3):290–4. [PubMed: 11850621]
34. Berkovich E, Monnat RJ Jr, Kastan MB. Roles of ATM and NBS1 in chromatin structure modulation and DNA double-strand break repair. Nat Cell Biol. 2007 Jun; 9(6):683–90. [PubMed: 17486112]
35. Lindgren M, Langel U. Classes and prediction of cell-penetrating peptides. Methods Mol Biol. 2011; 683:3–19. [PubMed: 21053118]
36. Milletti F. Cell-penetrating peptides: classes, origin, and current landscape. Drug Discov Today. 2012 Mar 23.
37. Kraakman-van der Zwet M, Overkamp WJ, Friedl AA, Klein B, Verhaegh GW, Jaspers NG, et al. Immortalization and characterization of Nijmegen Breakage syndrome fibroblasts. Mutat Res. 1999 May 14; 434(1):17–27. [PubMed: 10377945]
38. Cerosaletti K, Concannon P. Independent roles for nibrin and Mre11-Rad50 in the activation and function of Atm. J Biol Chem. 2004 Sep 10; 279(37):38813–9. [PubMed: 15234984]

39. O'Driscoll M, Cerosaletti KM, Girard PM, Dai Y, Stumm M, Kysela B, et al. DNA ligase IV mutations identified in patients exhibiting developmental delay and immunodeficiency. Mol Cell. 2001 Dec; 8(6):1175–85. [PubMed: 11779494]
40. Paull TT, Rogakou EP, Yamazaki V, Kirchgessner CU, Gellert M, Bonner WM. A critical role for histone H2AX in recruitment of repair factors to nuclear foci after DNA damage. Curr Biol. 2000 Jul 27; 10(15):886–95. [PubMed: 10959836]
41. Carson CT, Schwartz RA, Stracker TH, Lilley CE, Lee DV, Weitzman MD. The Mre11 complex is required for ATM activation and the G2/M checkpoint. EMBO J. 2003 Dec 15; 22(24):6610–20. [PubMed: 14657032]
42. Difilippantonio S, Celeste A, Fernandez-Capetillo O, Chen HT, Reina San MB, Van LF, et al. Role of Nbs1 in the activation of the Atm kinase revealed in humanized mouse models. Nat Cell Biol. 2005 Jul; 7(7):675–85. [PubMed: 15965469]
43. Horejsi Z, Falck J, Bakkenist CJ, Kastan MB, Lukas J, Bartek J. Distinct functional domains of Nbs1 modulate the timing and magnitude of ATM activation after low doses of ionizing radiation. Oncogene. 2004 Apr 15; 23(17):3122–7. [PubMed: 15048089]
44. Kitagawa R, Bakkenist CJ, McKinnon PJ, Kastan MB. Phosphorylation of SMC1 is a critical downstream event in the ATM-NBS1-BRCA1 pathway. Genes Dev. 2004 Jun 15; 18(12):1423–38. [PubMed: 15175241]
45. Uziel T, Lerenthal Y, Moyal L, Andegeko Y, Mittelman L, Shiloh Y. Requirement of the MRN complex for ATM activation by DNA damage. EMBO J. 2003 Oct 15; 22(20):5612–21. [PubMed: 14532133]
46. Matsuoka S, Rotman G, Ogawa A, Shiloh Y, Tamai K, Elledge SJ. Ataxia telangiectasia-mutated phosphorylates Chk2 in vivo and in vitro. Proc Natl Acad Sci U S A. 2000 Sep 12; 97(19):10389–94. [PubMed: 10973490]
47. Gatei M, Young D, Cerosaletti KM, Desai-Mehta A, Spring K, Kozlov S, et al. ATM-dependent phosphorylation of nibrin in response to radiation exposure. Nat Genet. 2000 May; 25(1):115–9. [PubMed: 10802669]
48. Lim DS, Kim ST, Xu B, Maser RS, Lin J, Petrini JH, et al. ATM phosphorylates p95/nbs1 in an S-phase checkpoint pathway. Nature. 2000 Apr 6; 404(6778):613–7. [PubMed: 10766245]
49. Wu X, Ranganathan V, Weisman DS, Heine WF, Ciccone DN, O'Neill TB, et al. ATM phosphorylation of Nijmegen breakage syndrome protein is required in a DNA damage response. Nature. 2000 May 25; 405(6785):477–82. [PubMed: 10839545]
50. Zhao S, Weng YC, Yuan SS, Lin YT, Hsu HC, Lin SC, et al. Functional link between ataxia-telangiectasia and Nijmegen breakage syndrome gene products. Nature. 2000 May 25; 405(6785): 473–7. [PubMed: 10839544]
51. Lukas C, Melander F, Stucki M, Falck J, Bekker-Jensen S, Goldberg M, et al. Mdc1 couples DNA double-strand break recognition by Nbs1 with its H2AX-dependent chromatin retention. EMBO J. 2004 Jul 7; 23(13):2674–83. [PubMed: 15201865]
52. Bekker-Jensen S, Lukas C, Kitagawa R, Melander F, Kastan MB, Bartek J, et al. Spatial organization of the mammalian genome surveillance machinery in response to DNA strand breaks. J Cell Biol. 2006 Apr 24; 173(2):195–206. [PubMed: 16618811]
53. Rouet P, Smih F, Jasin M. Introduction of double-strand breaks into the genome of mouse cells by expression of a rare-cutting endonuclease. Mol Cell Biol. 1994 Dec; 14(12):8096–106. [PubMed: 7969147]
54. Rouet P, Smih F, Jasin M. Expression of a site-specific endonuclease stimulates homologous recombination in mammalian cells. Proc Natl Acad Sci U S A. 1994 Jun 21; 91(13):6064–8. [PubMed: 8016116]

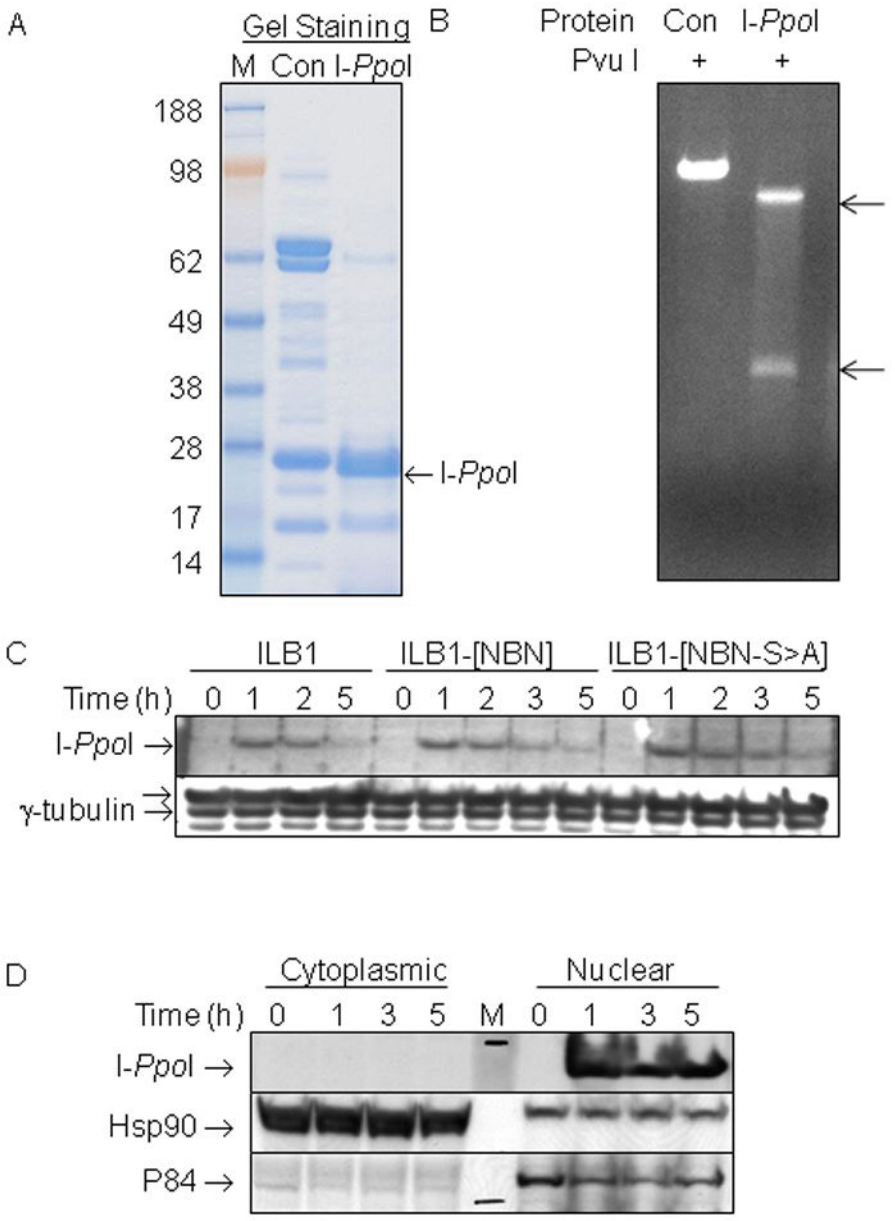

Figure 1.

I-*Ppo*I protein purification and transduction into human cells. (A) I-*Ppo*I protein purified from *E. coli* was detected by Coomassie staining. (B) pcDNA3.1 containing a synthetic I-*Ppo*I site was linearized by PvuI digestion, and incubated with either control (Con) protein (produced from pET45b(+) empty vector transformed cells) or purified I-*Ppo*I protein at 37°C overnight. Products were separated on agarose gel. (C) ILB1, ILB1-[NBN] or ILB1-[NBN-S>A] cells were transduced with purified I-*Ppo*I protein complexed with cell penetrating peptides (CPP). Cells were collected at 0, 1, 2, 3 and 5 hours after transduction. Total protein lysate was separated on a 4–12% gradient Bis-Tris gel, transferred to Immobilon-P transfer membrane and immunoblotted with a monoclonal anti-His antibody and a monoclonal anti-tubulin antibody respectively. (D) ILB1-[NBN] cells were transduced

with purified I-*Ppo*I protein complexed with CPP. Cells were collected at 0, 1, 3 and 5 hours after transduction. Cytoplasmic and nuclear fractions were prepared and separated on a 4–12% gradient Bis-Tris gel, transferred to Immobilon-P transfer membrane and immunoblotted with anti-His antibody, anti-Hsp90 (as a cytoplasmic control) and anti-p84 (as a nuclear control).

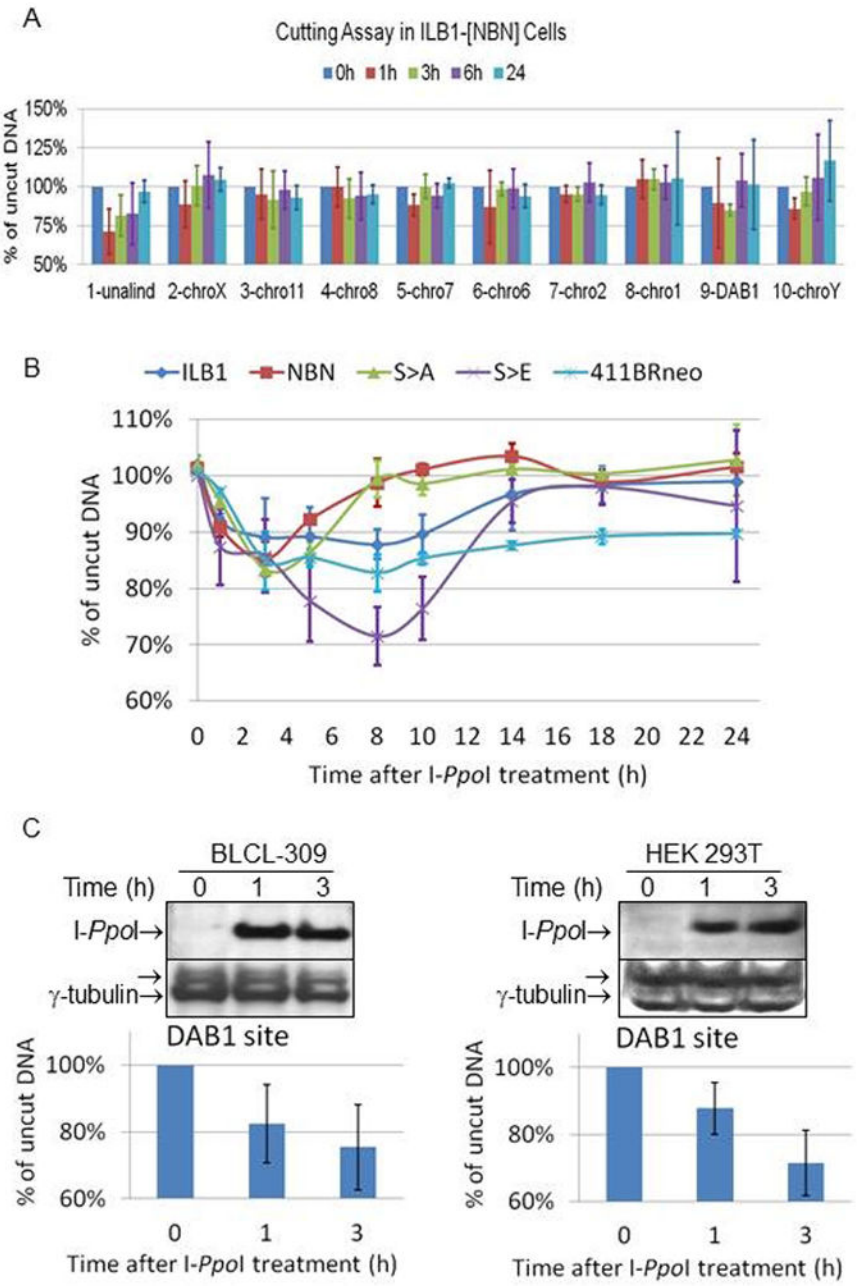

Figure 2.

Transduced I-*Ppo*I induces site-specific DNA cleavage in vivo. (A) In ILB1-[NBN] cells, the yield of PCR products spanning each of 10 identified I-*Ppo*I sites at different time points was compared with that from a reference sequence on chromosome 1 that did not contain an I-*Ppo*I site. Data were averaged from three independent experiments, and the error bars represent mean ± SD. (B) In ILB1, ILB1-[NBN], ILB1-[NBN-S>A], ILB1-[NBN-S>E] and 411BRneo cells, yield of PCR product at a single I-*Ppo*I site in the *DAB1* gene on chromosome 1 relative to a reference sequence lacking an I-*Ppo*I site on the same chromosome. The data represent the mean ± SD from independent triplicate experiments

each including two technical replicates. (C) In BLCL-309 and HEK293T cells, DNA and protein samples were collected at 0, 1 and 3 hours post I-*Ppo*I transduction. Yield of PCR product at a single I-*Ppo*I site in the *DAB1* gene on chromosome 1 was compared with that from a reference sequence on chromosome 1 that did not contain an I-*Ppo*I site (lower panel). Western blots show effective and rapid protein transduction (upper panel).

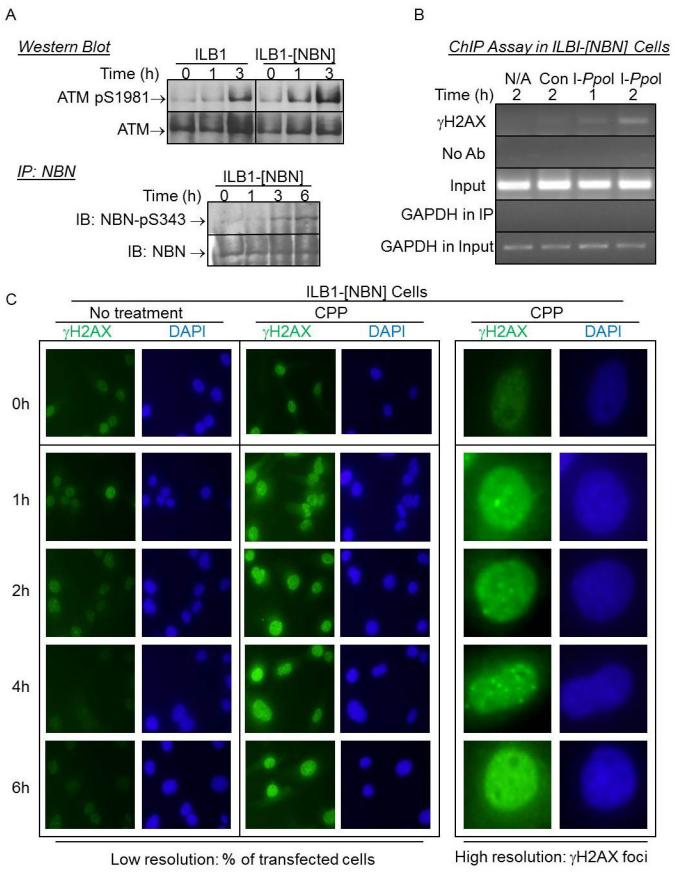

Figure 3.

I-*Ppo*I protein transduction activates ATM-dependent DNA damage responses. (A) In the upper panel, cells treated with I-*Ppo*I for the indicated amount of time were lysed, nuclear extracts were prepared and separated by 3–8% gradient gel, transferred to Immobilon-P transfer membranes, and immunoblotted with antibodies against ATM-phosphor-serine1981 (ATM-pS1981) and total ATM. In the lower panel, lysates from cells treated with I-*Ppo*I for the indicated times were immunoprecipitated with an anti-NBN antibody and immunoblotted with antibodies against NBN-phospho-serine343 (NBN-pS343) and total NBN. (B) ILB1-[NBN] cells were transduced with PBS (N/A), either control protein (Con) or purified I-*Ppo*I protein (I-*Ppo*I) using a protein delivery reagent (Chariot) and collected at 1 and 2 hours after transduction. ChIP assays were performed using either no antibody, or antibody against γH2AX. The immunoprecipitated DNA was quantitated by PCR using a primer set adjacent to the I-*Ppo*I site in the *DAB1* gene on chromosome 1 or primer set targeting a housekeeping gene, GAPDH. (C) ILB1-[NBN] cells were mock treated (No treatment), treated with CPP alone (CPP), or transduced with either control protein (Con-treated) or purified I-*Ppo*I protein (I-*Ppo*I-treated) complexed with CPP. Cells were fixed at 0, 1, 2, 4 and 6 hours after transduction and stained with γH2AX and DAPI. Low (20X) and high (40X) magnification images are shown for each time point.

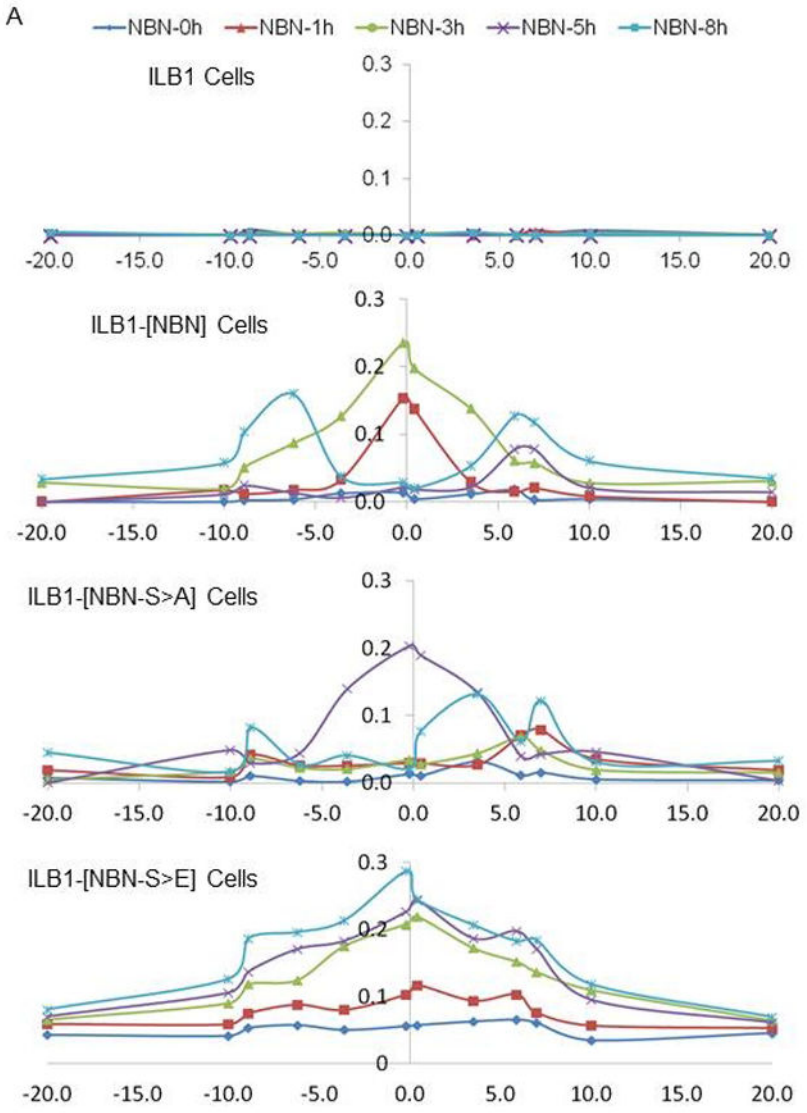

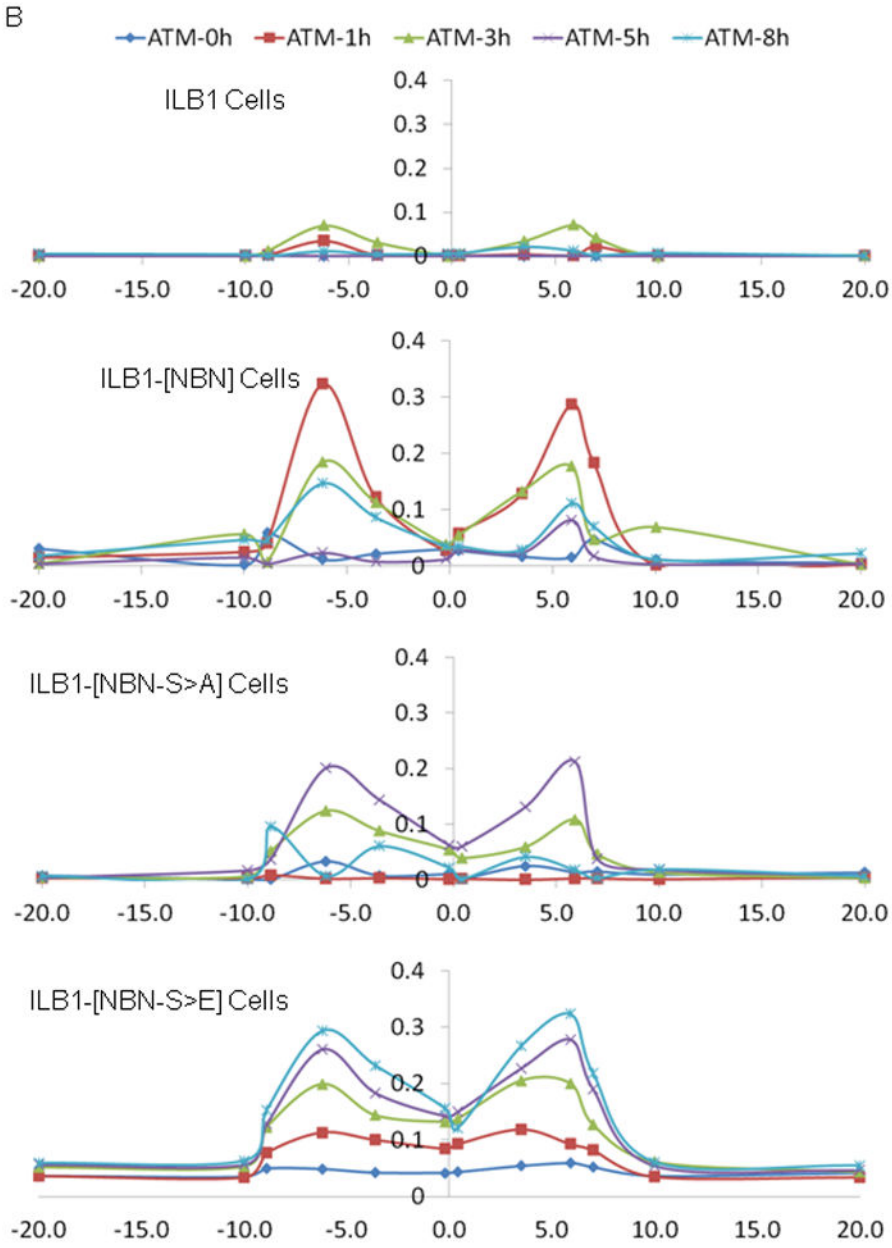

Figure 4.

Mutation of ATM phosphorylation sites on NBN alters the timing of ATM and NBN recruitment to the sites of damage. (A-B) ILB1, ILB1-[NBN], ILB1-[NBN-S>A] and ILB1-[NBN-S>E] cells were transduced with purified I-*Ppo*I protein using CPP. Cells were lysed at 0, 1, 3, 5 and 8 hours after transduction. ChIP assays were performed using antibodies against NBN (A), and ATM (B).

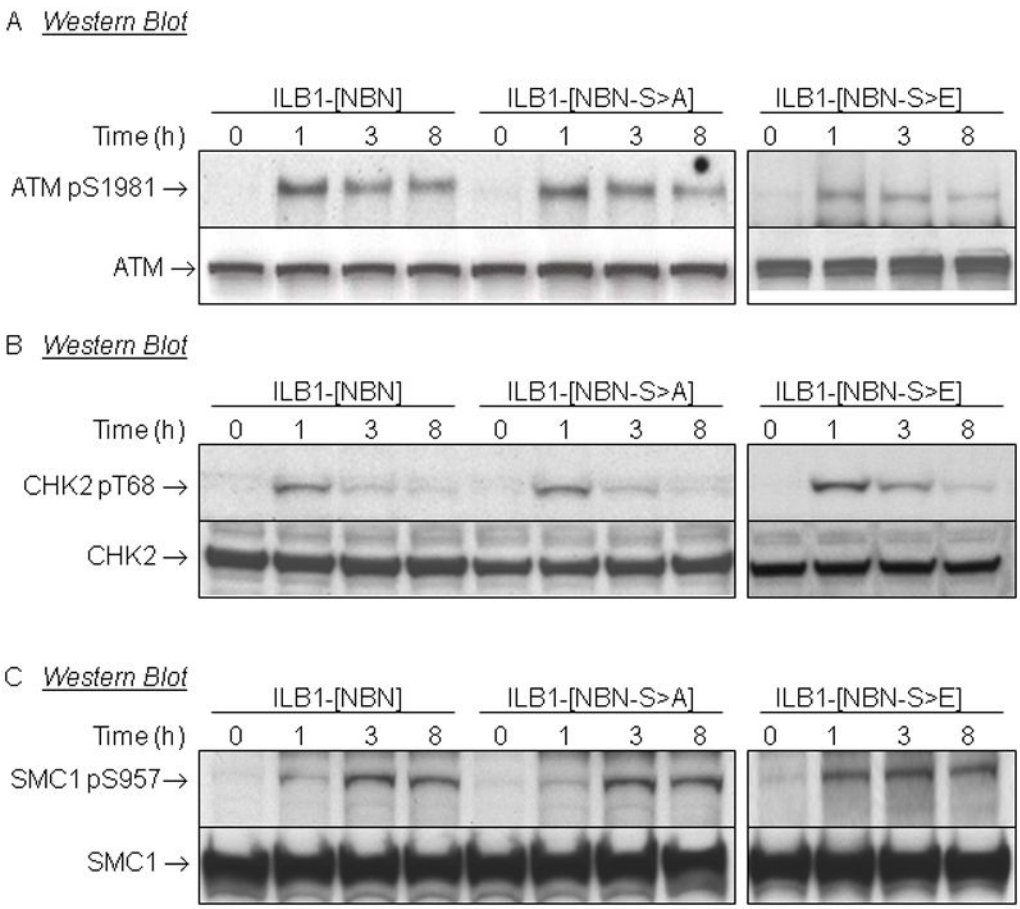

Figure 5.

Mutation of ATM phosphorylation sites on NBN does not alter the phosphorylation of ATM and its downstream effectors. (A) ILB1-[NBN], ILB1-[NBN-S>A] and ILB1-[NBN-S>E] cells were transduced with purified I-*Ppo*I protein and lysed at 0, 1, 3 and 8 hours after transduction. Nuclear extracts was prepared. Equivalent amounts of nuclear extract from the same preparation were separated on a 3–8% Tris-Acetate gel and a 4–12% Bis-Tris gel individually, transferred to Immobilon-P transfer membranes, and immunoblotted with antibodies against ATM-phosphor-serine1981 (ATM-pS1981, on Tris-Acetate gel), ATM (on Bis-Tris gel), (B) CHK2-phosphor-Tyrosine68 (CHK pT68, on Tris-Acetate gel) and CHK2 (on Bis-Tris gel), (C) SMC1-phosphor-Serine957 (SMC1 S957, on Bis-Tris gel) and SMC1 (on Tris-Acetate gel).